THE SECOND FORBIDDEN BETA TRANSITION OF COBALT 60

THE SECOND FORBIDDEN BETA TRANSITION OF COBALT 60

by

RASHIDA ALAM

A Thesis

Submitted to the Faculty of Graduate Studies

in Partial Fulfilment of the Requirements

for the Degree

Master of Science

McMaster University

April 1963

MASTER OF SCIENCE (1963)
(Physics)

McMASTER UNIVERSITY
Hamilton, Ontario

TITLE: The Second Forbidden Beta Transition of Cobalt 60

AUTHOR: Rashida Alam, M.Sc. (University of Dacca, Pakistan)

SUPERVISOR: Professor M. W. Johns

NUMBER OF PAGES: 37, v

SCOPE AND CONTENTS:

The 1.481 Mev second forbidden beta transition from the ground state of cobalt 60 to nickel 60 has been reinvestigated using the Siegbahn type spectrometer and discussed in this thesis. The end point energy, intensity and log ft values of the transition have been measured.

In addition, internal conversion peaks of two weak gamma transitions in nickel 60 have been observed. The experiment to find the energy and intensities of these transitions are described.

ACKNOWLEDGEMENTS

The author extends her deep appreciation to Professor M. W. Johns for his patient direction and kind encouragement during the course of this research.

The author wishes to express her gratitude to Dr. K. Fritze for his help in preparing the source.

Financial assistance from the Canadian Government in the form of a Colombo Plan Scholarship is gratefully acknowledged.

Thanks are also due to the members of the Beta and Gamma Ray Spectroscopy Group for their contributions to the success of this research and to Miss Patti Seigel for typing this thesis.

TABLE OF CONTENTS

LIST OF FIGURES

INTRODUCTION

Conflicting results exist in the literature regarding the second forbidden transition from the ground state of Co^{60} to the first excited state of Ni^{60} (part of the decay scheme is shown in Figure 1). Three groups of research workers have investigated this transition with varying results.

The first extensive work on the particular transition was done by Keister and Schmidt[1] at Washington University in 1954. They used a magnetic field solenoidal spectrometer and corrected the results for Compton electrons from high energy gamma fluxes in the sources. The high energy β-spectrum obtained from their results could not be fitted with the unique shape factor characteristic of $\Delta I = 3$, no, transition, and they made a fit of a $\Delta I = 2$, no, shape factor, assigning a spin of 4^+ for the ground state of Co^{60}. According to their fit, they calculated an intensity for the β-transition of 0.15%.

The same transition was later investigated by Wolfson[2]. He used a double lens magnetic spectrometer and lowered the background counting rate by pulse height selection. The effect of source thickness and the gamma background was reduced by restricting the region studied to that portion of the β-spectrum of energy greater than that of the γ-rays emitted from the source.

Wolfson's results differ from that of Keister and Schmidt. He claimed that the high energy β-group could be fitted with the unique

twice forbidden shape factor ($\Delta I = 3$, no) in accord with the experimental results that the spin of the ground state of Co^{60} is 5^+. The energy of the transition was 1.478 Mev, but the relative intensity was only 0.01%. The log ft value, which expresses the matrix elements operative in β-decay, was calculated as 12.8.

Camp, Langer and Smith[3] worked on the same problem at Indiana University. They used a 40 cm radius of curvature, shaped magnetic spectrometer and a strong 15 mc source. They analyzed the part of the β-spectrum between the 1.17 and 1.33 Mev conversion lines and also in the short stretch of the spectrum beyond those. The shape of the spectrum they found to be consistent with that expected for a unique twice forbidden transition, from 5^+ to 2^+ level, although they suggested $\Delta I = 2$, no, spectrum could not be completely ruled out. The relative intensity of this transition they found to be 0.12%, when compared directly with the intense β group and the log ft value was 11.8.

In the present work, the high energy β-group in the decay of Co^{60} has been re-investigated and the value of the percentage of its occurrence has been found. Moreover, the internal conversion peaks for two weak gamma rays in Ni^{60} have been observed. This thesis describes the study of the β-spectrum and the internal conversion peaks. However, before the experimental work is described, a short discussion of theoretical and experimental concepts necessary for the understanding of the experimental work has been presented. The appendix gives a brief account of the calculation of the shape factors required for the work.

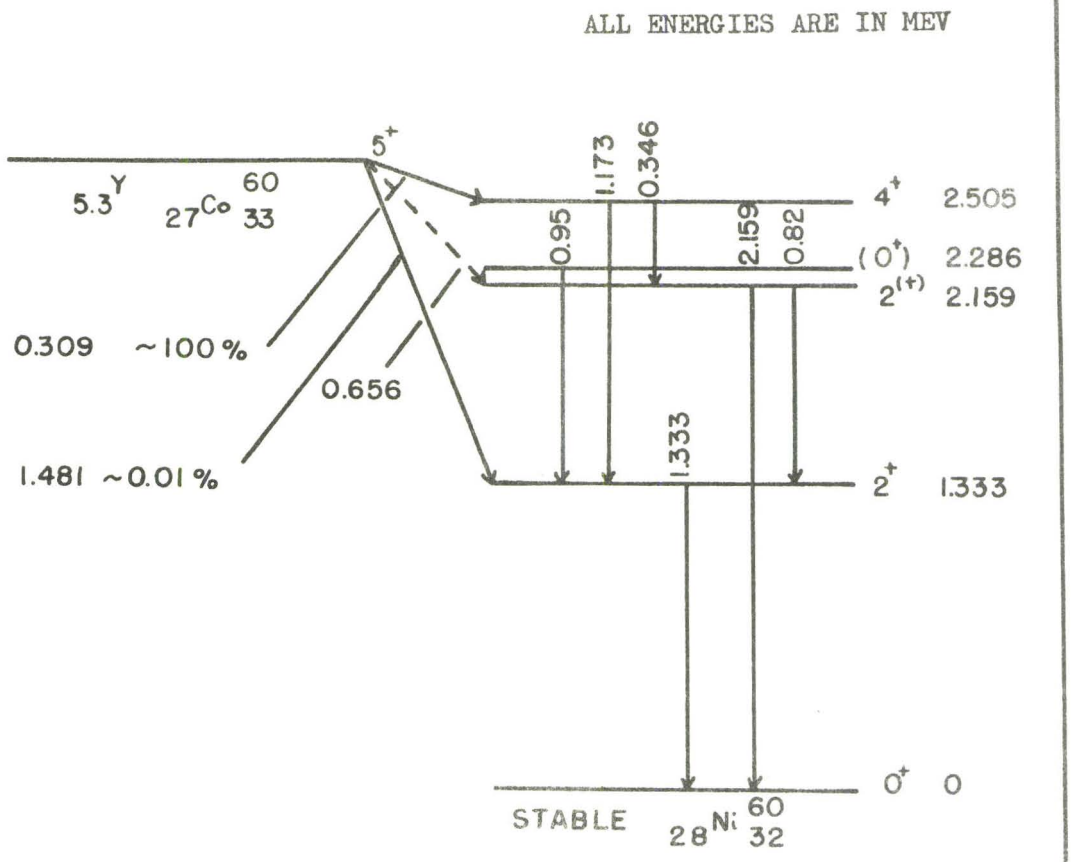
ALL ENERGIES ARE IN MEV
5+
5.3Y
27Co 60 33
0.309 ~100%
0.656
1.481 ~0.01%
1.173
0.346
0.95
2.159
0.82
1.333
4+ 2.505
(0+) 2.286
2(+) 2.159
2+ 1.333
0+ 0
STABLE
28Ni 60 32

FIGURE 1

THEORY OF BETA-DECAY AND INTERNAL CONVERSION

Beta-Decay

In general, the beta-decay processes are to be described as nuclear transitions between states of equal mass number in which certain light particles are emitted, absorbed or both. The process involves one of the following three forms: e^- emission, e^+ emission or orbital electron capture. To conserve the energy, momentum and statistics in the beta decay process, the neutrino, which is a lepton of zero mass, no charge and 1/2 integral spin, was first postulated by Pauli in 1927 and experimentally verified by Reines and Cowan in 1953. In 1934, Fermi[4] worked out a theory of beta-decay consistent with the experimental results. This mechanism, which allows for the emission of two particles with the total energy shared by them in a statistical manner, predicted a beta-continuum of proper shape and suggested that the end point of the continuum was associated with the energy released of the beta-process.

The probability of occurrence of a beta-process in which an energy E is released in a system with initial state i and final state f is given by

$$P(E) = \frac{2\pi}{\hbar} \left| H_{if} \right|^2 \frac{dn}{dE} \quad \text{where } \frac{dn}{dE} \text{ is the}$$

density of the final states and H_{if} is the matrix element of the interaction.

$$H_{if} = g \int \left[U_f^* \varphi_e(r) \varphi_\nu(r) \right] O_x U_i \, dv \qquad (1)$$

where g is the interaction constant, U_i and U_f the wave functions of the nucleus before and after the interaction, $\varphi_e(r)$ and $\varphi_\nu(r)$ describe the electron and neutrino respectively, and O_x is the interaction operator.

In Fermi's original theory it was suggested that O_x may take the form of one or a mixture of several of five possible interactions - scalar, vector, tensor, axial vector and pseudoscalar. But since it is proved that, in beta-decay parity is not conserved and both electron and neutrino are left handedly polarized, beta-decay takes place only through a vector and/or axial vector interaction.

Allowed and Forbidden Transitions

Expanding the leptonic wave functions in terms of increasing angular momentum and decreasing magnitude in relation (1) and accepting only the first terms in these experiments, we get, for electron momentum between p and p + dp,

$$P(p)\,dp = K \left| M_{if} \right|^2 F(Z,E)\, p^2\, (E_o - E)^2\, dp \qquad (2)$$

where $$M_{if} = \int U_f^*\, Q_x\, U_i\, dv.$$

The Q_x are the approximate forms of O_x, E and E_o refer to total electron energy and total energy released in the decay respectively and K is a constant proportional to the interaction strength. F (Z,E) is the Coulomb correction factor (Fermi function) which may be included to allow for the effect of Coulomb forces on the electron created in the nuclear process. E and E_o are customarily expressed in $m_o c^2$ units and include the rest mass of the electron.

For a source of strength N_o disintegrations per second, the number of disintegrations N (p), with momentum between p and p + dp

will be $N_o P(p)\,dp$. So equation (2) can be written as

$$\sqrt{\frac{N(p)}{p^2 F(Z,E)\,dp}} \propto (E_o - E).$$

With magnetic spectrometers, the acceptance window $\Delta p = Rp$, where R is defined as the resolution of the spectrometer and is constant for any given combination of slit width, detector width and baffle settings.

Therefore,

$$\sqrt{\frac{N(p)}{p^3 F(Z,E)}} \propto (E_o - E).$$

It is convenient to use the tabulated[5] function $G = pF/E$ in computing

$$\sqrt{N(p)/p^3 F}.$$

In terms of G, this expression becomes

$$\sqrt{\frac{N(p)}{p^2 EG}} \propto (E_o - E) \qquad (3)$$

A graph of the left hand side of the above expression against E should be a straight line with intercept on the E axis at E_o, the maximum energy released in the transition. Thus the use of the so-called Fermi plot yields a precise method of finding E_o.

Integrating equation (2) over the total energy spectrum, the total probability of β-decay is given by

$$\lambda = \int_0^{p_{max}} P(p)\,dp = \frac{0.693}{t} = K\left|M_{if}\right|^2 \int F(Z,E)\, p^2 (E_o - E)^2\,dp$$

$$= K\left|M_{if}\right|^2 f(Z,E_o).$$

$$\text{or} \qquad ft \propto \left|M_{if}\right|^{-2} \qquad (4)$$

where t is the half life. Using the tabulated values of f (Feenberg) for different values of Z, ft values give the information about nuclear matrix element M_{if}.

For allowed transitions, the vector form of the interaction operator leads to Fermi selection rules $\Delta I = 0$ and no parity change. The axial vector operator leads to the Gamow-Teller selection rules $\Delta I = 0 \pm 1$, $0 \not\rightarrow 0$ and no parity change.

In practice, transitions which are not allowed by the above mentioned selection rules may also occur. This suggests the need of corrections for the exact form of the matrix element and higher order terms in the leptonic wave function expansion. If the matrix element containing the first term of the expansion vanishes, one has to consider the second term which leads to the transition known as the first forbidden. With the third term leading to a non-vanishing matrix element gives a second forbidden transition and so on.

With the above corrections, equation (2) becomes

$$P(p)\,dp = K \left| M_{if} \right|^2 F(E,Z)\, p^2\, (E_o - E)^2\, Sn(E) \qquad (5)$$

where Sn (E) is the shape factor for the forbidden spectrum of degree n. In this case, the Fermi analysis requires that

$$\left[N(p) \,/\, F(Z,E)\, p^2\, Sn(E) \right]^{1/2}$$

be plotted against E to get a straight line. As before, the intercept of the straight line obtained with the energy axis gives the value of the maximum energy of the β-disintegration.

In summary, vector and axial vector operators involved in β-decay now lead to the following selection rules.

	Vector (Fermi)	Axial Vector (Gamow-Teller)
Allowed	$\Delta I = 0,\ \Delta\pi = \text{No}$	$\Delta I = 0, \pm 1,\ \Delta\pi = \text{No}$ $0 \not\to 0.$
First Forbidden	$\Delta I = 0, \pm 1,\ \Delta\pi = \text{Yes}$ $0 \not\to 0$	$\Delta I = 0, \pm 1, \pm 2,\ \Delta\pi = \text{Yes}$
Second Forbidden	$\Delta I = 0, \pm 1, \pm 2,\ \Delta\pi = \text{No}$ $0 \not\to 0$ $1 \not\to 0$	$\Delta I = 0, \pm 1, \pm 2, \pm 3$ $\Delta\pi = \text{No}$ $0 \not\to 0$ $1 \not\to 0$ $1 \not\to 1$
etc.		

Certain Gamow-Teller interactions of nth forbiddenness involve $\Delta I = n + 1$ and are known as the nth unique forbidden transitions. The first forbidden unique interaction has $\Delta I = 2$ and $\Delta\pi = \text{Yes}$ (eg. Y^{91}) for which $S_1(E) \simeq p_e^2 + p_\nu^2$. Similarly, there are unique second forbidden (Be^{10}, $\Delta I = 3$, No) and unique third forbidden (K^{40}, $\Delta I = 4$, Yes) transitions, with shape factors of the form $p_e^4 + 10/3\ p_e^2\ p_\nu^2 + p_\nu^4$ and $p_e^6 + 7\ p_e^4\ p_\nu^2 + 7\ p_e^2\ p_\nu^4 + p_\nu^6$ respectively (the general expression for the shape factors due to Greuling[6] and Konopinsky[7] is given in the appendix). Since in these cases the interaction is of pure vector type it has been possible to calculate the shape factors involved exactly. In more general cases of higher order forbidden, non-unique transitions, the shape factors cannot be calculated without a knowledge of the exact interaction form.

For a forbidden transition, the ft-value is not a direct measure of nuclear matrix element but involves the shape factor too. Consequently the value gives an indication of the order of forbiddenness of a spectrum. The general expression for f_n of the ft value of a nth forbidden transition is given by

$$f_n = \int_1^{E_o} S_n F(E,Z)\, pE\, (E_o - E)^2\, dE$$

where E_o is the end point energy + $m_o c^2$.

However, the complexity of the correction terms S_n makes most calculations difficult.

A very great simplification is obtained if one considers the unique forbidden transitions where one can calculate the exact form of the shape factors. It has been shown by Davidson[8] that using the appropriate form of the shape factors, the general expression for f, for a nth unique forbidden transition can be expressed as

$$f_n = \bar{S}_n (E_o)\, f_o \qquad (6)$$

where f_o refers to the same quantity for allowed transitions,

$$f_o = \int_1^{E_o} F(E,Z)\, pE\, (E_o - E)^2\, dE$$

and $\bar{S}_n$ are

$$12\, \bar{S}_1 (E_o) = (6/10)(E_o^2 - 1) - (1/5)(E_o - 1),$$

$$5 \times 6^3\, \bar{S}_2 (E_o) = (3/7)(E_o^2 - 1)^2 - (26/105)(E_o^2 - 1)(E_o - 1) - (2/105)(E_o - 1)^2,$$

and $$70 \times 70^2\, \bar{S}_3 (E_o) = (1/3)(E_o^2 - 1)^3 - (9/35)(E_o^2 - 1)^2 (E_o - 1) - (2/35)(E_o^2 - 1)(E_o - 1)^2 + (8/105)(E_o - 1)^3. \qquad (7)$$

Using Feenberg and Trigg's[9] curves for log f_o against Z, and the above expressions for $S_n(E_o)$, ft values for the first, second and third forbidden unique transitions can be readily calculated.

Since ft-values vary over a wide range, it is customary to quote $\log_{10}$ft, and to measure the half-life in seconds. It has been shown that matrix elements of successive order of forbiddenness differ by factors of order about 10^{-2}, so that changes of 4 or 5 in log ft should not be unexpected. From the form of the shape factors of unique forbidden transitions, it can be predicted that the log ft values for unique spectra may be greater by about 2 than the values for other transitions of the same order. While the allowed transitions have log ft values between 3 and 6, the first forbidden transitions with $\Delta I = 0$ or 1 have log ft near 7. The first forbidden unique transitions have values around 9, although there are some as low as 7 and as high as 10. The second forbidden transitions have log ft between 12 and 14. The third forbidden log ft values cluster close to 18 and the one example of a fourth forbidden transition, In^{115}, has log ft = 23.02.

Internal Conversion

Internal conversion is a process competing with gamma emission in de-exciting the nucleus. In this process the de-excitation energy of the nucleus is transferred to one of the orbital electrons which subsequently leaves the atom. The energy of the emitted electron is $E_e = E_\gamma - E_\beta$ where E_γ is the energy released by the nucleus and E_β is the binding energy of the shell from which the electron is emitted. The process can occur even when gamma emission is completely forbidden as in the electric $0 \longrightarrow 0$ monopole transition.

The ratio of the internal conversion probability in a shell S to the gamma emission probability is called the internal conversion coefficient of the shell and has been calculated for a number of shells. This ratio is defined as

$$\alpha_s = \frac{Ne_S}{N_\gamma}$$

and total conversion coefficient is

$$\alpha = \sum_S \alpha_S .$$

In certain cases, requisite information can be obtained from relative conversion coefficients for different shells or subshells. Thus one refers to K/L and L_1/L_2 ratios which are defined as

$$N_{eK}/N_{eL} = \alpha_K/(\alpha_{L_1} + \alpha_{L_2} + \alpha_{L_3}),\ N_{eL_1}/N_{eL_2} = \alpha_{L_1}/\alpha_{L_2} \text{ etc.}$$

All these ratios depend on the multipolarity of the radiation and the parity change. A study of internal conversion is one of the most useful procedures for the classification of nuclear energy levels.

The conversion coefficients first calculated and tabulated by Rose, assumed the nucleus to be a point charge and the nuclear matrix elements do not enter into the calculations. Later, he made corrections in his results, considering the electron wave function different from that due to a point nucleus. L. A. Sliv[19] considered a further correction for the fact that the electron spends part of its time inside the nucleus and thus the positions and motions of nuclear charges are important. Except for certain nuclei, both sets of calculations give essentially the same results and Rose's tables have been used in the present work.

THE BETA-RAY SPECTROMETER

The experiment was carried out with the high resolution Siegbahn type double focussing spectrometer. The construction and performance of the instrument has been described by Johns et al[10].

Description of the Instrument

The spectrometer is a modified semicircular instrument in which the magnetic field is made inhomogeneous in such a way as to provide both radial and axial focussing of electrons from the source. To achieve this, the axial component of the field, expressed in the nomenclature of Schull and Dennison[11], is given by

$$H(r, z) = H_o \left[1 - \frac{1}{2} \left(\frac{r-a}{a}\right) + \beta \left(\frac{r-a}{a}\right) - \left(\frac{4\beta - 1}{4a^2}\right) z^2 + .. \right] \quad (8)$$

where H_o refers to the axial field on $r = a$, $z = 0$ circle. β is a second order focussing parameter and equal to 5/8 in our instrument. In such a field the electron trajectories inside a certain solid angle Ω will cross at approximately $\phi = \pi\sqrt{2}$ (254°).

A sketch of the instrument is shown in Figure 2. The magnetic pole faces are of Armco iron with the magnet coil consisting of 10,000 turns of No. 18 formex wire wound in 8 pies. The vacuum chamber at 50 cm radius is of 1/4" aluminum sheet with both ends closed with sliding brass gates, which permit the source and detector assemblies to be changed easily and positioned accurately on the 50 cm circle. The

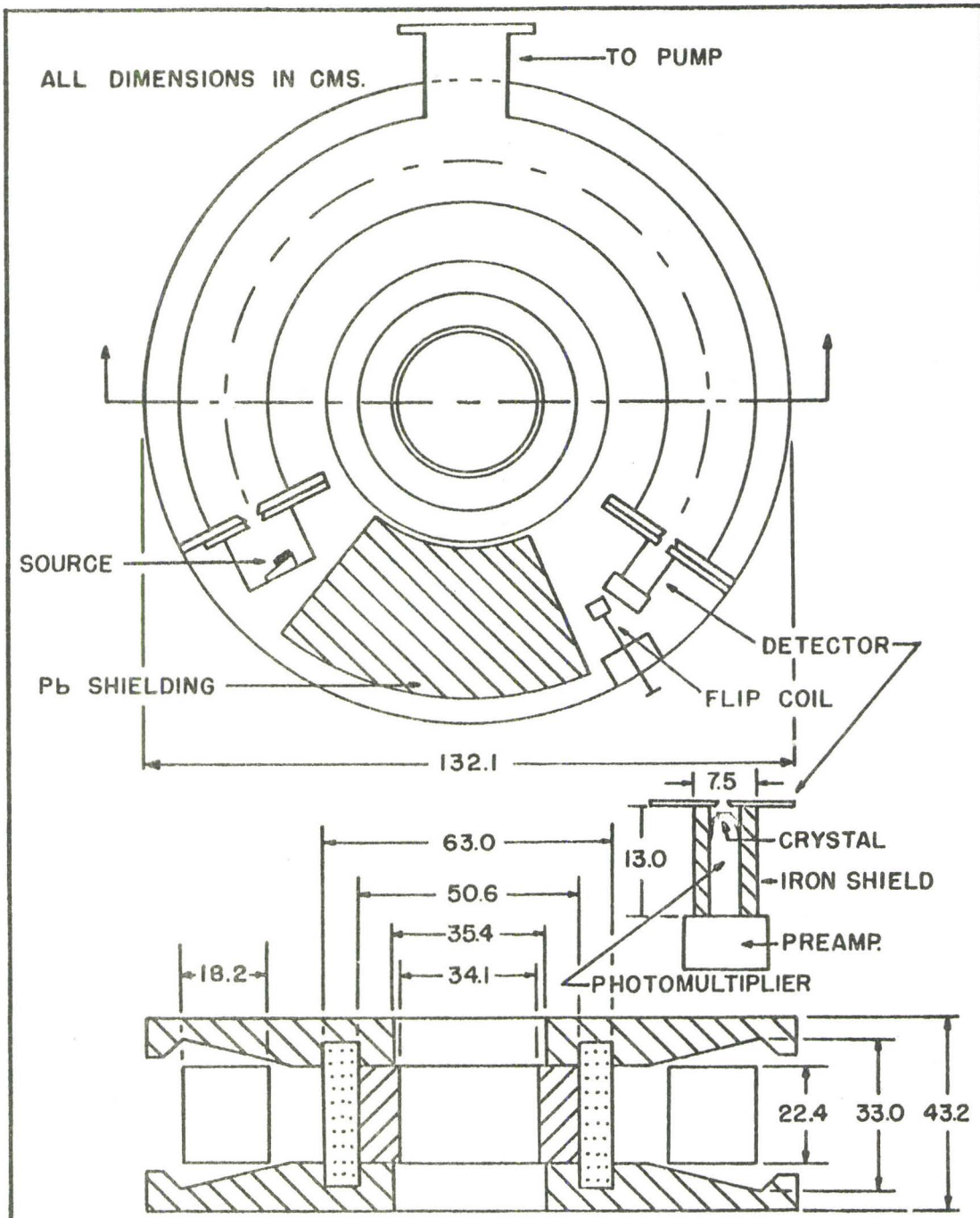

HIGH RESOLUTION BETA-RAY SPECTROMETER

FIGURE 2

electron beam is defined by a set of baffles provided at 30°, 60°, 118°, 155°, 194° and 224° positions in the vacuum chamber. An additional set of horizontal and vertical baffles provided at 40° can be adjusted for maximum resolution.

In normal operation, the pressure in the chamber is maintained at a value somewhat below 0.1 microns which is provided by a water-cooled metal oil diffusion pump of capacity 100 litres per second and a Cenco Megavac fore-pump.

The current is provided by a stabilized power supply, supplying 850 ma at 750 v with a current stability of about 0.01%. The current can be varied by a ten-position selector switch with the fine adjustment being made with a ten-turn helipot.

The magnetic field is measured by means of a flip coil and a Leeds and Northrup type R galvanometer, with a lamp and scale distance of 2 meters. The flip coil has a variable number of turns (100, 75, 45, 25, 10).

The source is introduced into the spectrometer through a vacuum gate consisting of a brass plate which slides over the flat end of the vacuum box. To this plate is attached the assembly holding the source. The source assembly has to be pumped out before connecting to the vacuum chamber. The detector assembly is attached to another sliding gate at the other end of the vacuum chamber. The detector used consists of a 1 cm x 2.4 cm x 1 cm plastic crystal and a duMont 6292 photomultiplier tube which is shielded by a cylinder of Armco iron. In front of the detector there is a set of slits which can be varied from 1 mm to 7 mm.

Response of the Spectrometer to a Monoergic Electron Beam

To describe the response of a spectrometer to a monoergic electron beam of finite angular spread emerging from a source of finite area, we may introduce a function $g(\xi, p)$ which is the probability of recording an electron of momentum ξ when the instrument is set to focus electrons of momentum p. If $\xi = p$ the value of g is unity. It can be shown that $g(\xi, p)$ is independent of p and depends only on $(\xi - p)/p$. Hence, writing $(\xi - p)/p = u$, we have

$$\int_0^\infty g(\xi, p)\, d\xi = p \int_0^\infty g(u)\, du = p\eta,$$

where η is a constant for a given spectrometer and depends only on the source, detector and baffle geometry.

If a monoergic source of electrons of intensity N_o is placed in the spectrometer, the detector counting rate $N(p)$, at an arbitrary value of p is $N(p) = N_o \omega g(\xi_o, p)$ and the peak counting rate is $N_o\omega$. If we now plot N/p vs p, the area under the peak is

$$\int_0^\infty \frac{N(p)}{p}\, dp = \omega N_o \int_0^\infty \frac{g(\xi_o, p)\, dp}{p},$$

where ω is the solid angle subtended by the detector.

However, since $g(\xi, p)$ vanishes unless $p \cong \xi_o$, the effective range of integration is so small that we can remove p from under the integral sign. Hence

$$\int_0^\infty \frac{N(p)}{p}\, dp = \frac{\omega N_o}{p} \int_0^\infty g(\xi, p)\, dp$$

$$= \omega N_o \eta.$$

In spectrometers where the peak profile is symmetric, η will be very nearly equal to the resolution $R = \Delta p/p$. This condition is satisfied for the Siegbahn type spectrometer.

When the peak obtained is due to the conversion electrons for a γ-transition,

$$\int_0^\infty \frac{N(p)}{p}\, dp = \omega N_o R. \frac{\alpha}{1+\alpha} .I. \qquad (9)$$

where α is the conversion coefficient and I the intensity of the transition.

Response of the Spectrometer to a Continuous Distribution

For a beam of electrons of continuous energy distribution, we introduce a factor $\phi(\xi)$ which is the probability per electron that the momentum will lie in a unit interval of momentum about ξ,

$$\int_0^\infty N_o \phi(\xi)\, d\xi = N_o$$

where N_o is the source strength. When the spectrometer is set at p, the counting rate is

$$\int_0^\infty N_o \phi(\xi)\, g(\xi, p)\, \omega d\xi .$$

We may now put $\phi(\xi) = \phi(p)$ = constant over the range of integration and the counting rate becomes

$$N_o \phi(p)\, \eta p \omega .$$

If N (p)/p is plotted against p, the area under the curve is given by

$$\int_0^\infty \frac{N(p)}{p}\,dp = \int_0^\infty \frac{N_o \phi(p)\,\eta p\omega\,dp}{p} = N_o \eta\omega \simeq N_o R\omega.$$

When the branching ratio of the β-spectrum is f, the area under the curve is given by

$$\int_0^\infty \frac{N(p)}{p}\,dp = N_o R\omega f. \qquad (10)$$

Measurement of β and γ Intensities with the Spectrometer

Measurement of β-Intensity

Comparison of the areas under the beta spectrum and a conversion peak measured with the same instrument and from the same source gives

$$\frac{\text{Area under the β-spectrum}}{\text{Area under the conversion peak}} = \frac{f(1+\alpha)}{\alpha . I} \qquad (11)$$

where the terms are explained in the previous section.

Experimental measurement of the areas under the β-spectrum and the conversion peak together with the knowledge of α and I, therefore gives a measurement of f, the intensity of the β-spectrum.

Measurement of γ-Intensity

Since α, the internal conversion coefficient is defined as $Ne/N\gamma$, the total number of transitions from an excited level (not undergoing a β-transition) is given by

$$\frac{Ne}{\alpha} + Ne.$$

If the intensity of the transition is given by I, the intensity, I', of any other transition in the particular nucleus is given by

$$I' = \frac{\frac{Ne'}{\alpha'} + Ne'}{\frac{Ne}{\alpha} + Ne} \times I \qquad (12)$$

where Ne' and α' are the number of internal conversion electrons and conversion coefficient respectively, of the transition whose intensity is sought.

THE SOURCE PREPARATION

A pellet of active Co^{60} coated with nickel was received from Chalk River. The pellet had a specific activity of about 167 curies/gm. The contained curie content was about 1.2 curies and handling this large amount of activity required special care.

To dissolve a portion of the pellet the following method was adopted. A glass tube (of about 8 mm in inner diameter) bent in the manner shown in Figure 3 had a polythene tube connected to one end. About half way down the tube a perforated glass disc was fitted and the lower free end of the polythene tube was dipped in dilute nitric acid kept in a beaker. Heavy shielding was provided around the tube which was viewed through a mirror placed above.

The active cobalt pellet was then slid from the aluminum shipping container into the tube and dropped in position on the glass disc behind the shielding. With a rubber atomizer fitted at the upper end of the glass tube, some nitric acid was sucked up to the cobalt pellet and allowed to react with the cobalt. After two minutes the acid solution was collected in a new beaker. Practising previously with similar pellets of inactive cobalt showed that in the process about 10% of the contained metal was dissolved in the acid.

The active solution was now slowly evaporated to dryness. In order to prepare a cobalt chloride solution two ml of half-normal hydrochloric acid was then added to the beaker and the solution evaporated

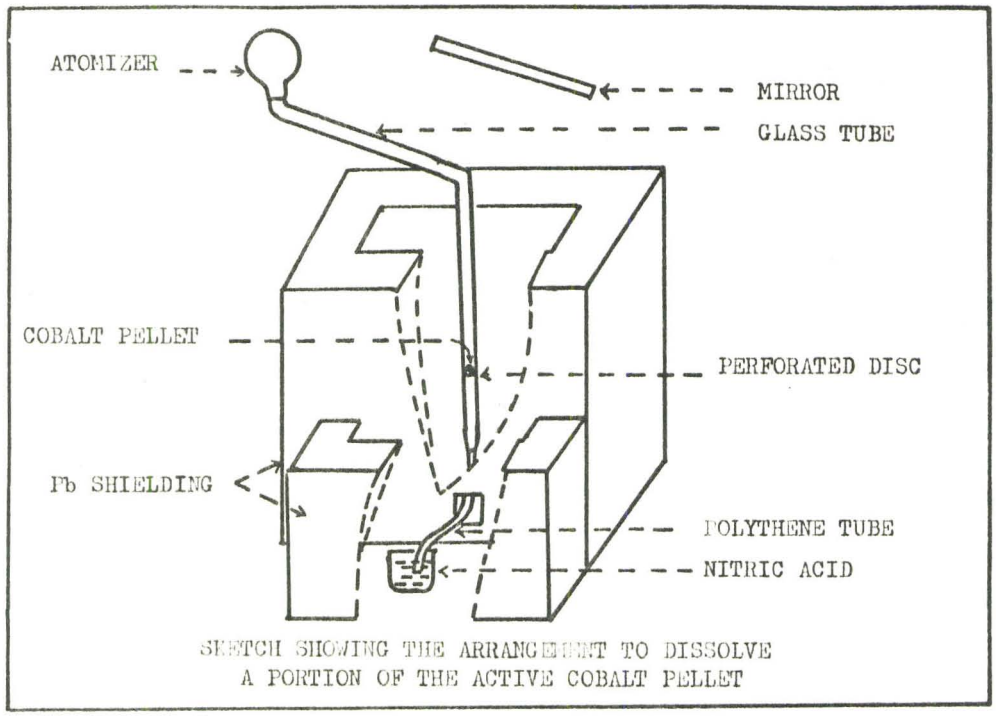

SKETCH SHOWING THE ARRANGEMENT TO DISSOLVE
A PORTION OF THE ACTIVE COBALT PELLET

FIGURE 3

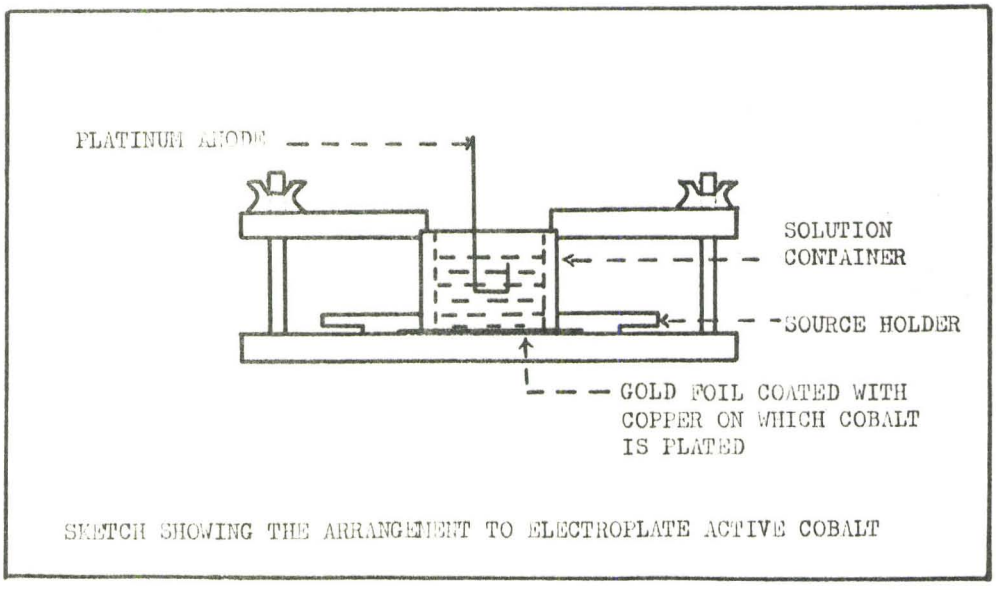

SKETCH SHOWING THE ARRANGEMENT TO ELECTROPLATE ACTIVE COBALT

FIGURE 4

again. To the cobalt chloride crystals thus prepared were added two ml of a boric acid solution prepared in the following manner[12]. A 4.5% boric solution was first prepared. To every 50 ml of this solution was added 0.25 mole of sodium chloride and 0.25 mole of cobalt chloride and the pH then adjusted to 3 by adding dilute hydrochloric acid or sodium hydroxide.

A thin layer of copper was electroplated[13] on a piece of mylar foil coated with gold. The foil was placed below a jig which pressed the copper plated surface against the bottom of a container (Figure 4). The plating solution was pipetted into the container and a platinum wire anode was dipped into the solution. Passing a current of 15 ma for three hours removed almost all the cobalt from the plating solution and plated it on a surface area 2 cm x 0.5 cm.

It would have been desirable to mount the source on a thinner backing but it was necessary to be certain that the Co^{60} activity was firmly bound to the backing material because of the danger of contaminating the spectrometer. It was found by trial and error, using inactive cobalt, that the cobalt deposit would not adhere to aluminum mylar nor to the gold coated mylar. However, it was possible to copper plate the gold surface and then plate a tightly adhering and uniform cobalt layer on this copper. The total backing thickness amounted to 0.6 mg/cm^2 of mylar, 0.1 mg/cm^2 of gold and 0.1 mg/cm^2 of copper. The source itself had a thickness of 0.6 mg/cm^2.

EXPERIMENTAL DETAILS AND DISCUSSION

The source was carefully introduced in the spectrometer and the high energy β-spectrum was followed to the end point including the sharp internal conversion peaks of the 1.172 and 1.332 Mev gamma-rays. The spectrum below and in between the peaks was liable to give erroneous results due to electrons scattered from the spectrometer slits and walls and so more attention was paid to the short stretch of the spectrum beyond the 1.332 Mev conversion peak.

Setting the instrument at the high energy tail of the spectrum and passing a reverse current in the magnet showed a background counting rate of about 26 counts/min. Since the actual number of counts in this region was very low, it was necessary to reduce the background count as much as possible. A pulse height analyzer was not used for fear it might discriminate against some of the desired electrons. So the background was lowered by the three following adjustments.

In the first place, a heavier wall of lead blocks was inserted around the detector to reduce the background to about 15 counts/min. In the second place, the high voltage (HT) on the photomultiplier tube was reduced as much as possible consistent with 100% detection of the K-conversion line of the 1.332 Mev transition. This method reduced the background to about 5 counts/min near the expected end point of the beta-spectrum.

The background was further lowered by defining the beam with the variable baffles. This adjustment lowered the number of electrons scattered from the inner walls of the spectrometer. While the horizontal baffles were not of much help in lowering the background, closing the vertical baffles a suitable position brought the background down to about 3.5 counts/min. The resolution of the instrument at this position of the baffles was about 0.5%. The detector slit was kept at 7 mm.

With the above setting of the instrument, the beta-spectrum was followed in between the conversion peaks and beyond, up to the end point. The conversion lines of the 1.172 Mev and 1.332 Mev gamma-rays and the portions of the β-spectrum are shown in Figure 5.

The beta spectrum was subjected to a Fermi analysis and the conventional Fermi plot without any shape factor is shown in the inset of Figure 5. The data in the region of the beta-spectrum between the conversion peaks could not be fitted smoothly to the data in the high energy tail of the spectrum. The counting rate in this region was too high, possibly due to the secondary electrons from the source backing and the spectrometer chamber and therefore was not used in calculating the final results.

The Fermi plot is re-plotted as Line I in Figure 6. The line shown is a least squares fit to the data. It is noted that the fit is not very good at high energies and that the end point of 1.487 Mev is 6 kev above the value predicted from the well known portions of the decay scheme. Moreover, the data suggests that the Fermi plot is not really linear and should not have been fitted to a straight line.

Curve II represents a least squares fit to the same data when the shape factor for a $\Delta I = 3$, no transition is included. The end point

of this curve falls at 1.479 Mev, in good agreement with the value of 1.481 $\pm$ 0.003 Mev predicted from the decay scheme. The sum of the squares of the residuals for Curve II is 1.22×10^{-6} against the much larger value 4.27×10^{-6} of Curve I.

There is a possibility that the particular beta transition implies $\Delta I = 2$, no parity change for which the ground state of Co^{60} has a spin 4^+. The attempt to calculate the shape factor for this second forbidden non-unique transition is given in the appendix. The appropriate value of λ in the shape factor $(E_o^2 - 1) + \lambda (E_o - E)^2$ requires knowledge of the wave functions of the initial and final states of the transition. Without going into the details of the calculation, the possible approximate values of λ are chosen, as shown in the appendix. The Fermi plots for the shape factors with λ of the order of unity are almost coincident and shown as Curve III in Figure 6. The Curve IV is that with λ around 100. It is difficult to conclude anything definite from these curves because of the short energy range of the data and the arbitrariness of the value of λ. The nuclear shell model indicates a spin of 5^+ for the ground state of Co^{60} and this choice of spin is also strongly suggested by the Co^{60} alignment and paramagnetic resonance hyperfine structure experiments[14]. The second forbidden unique transition is, therefore, considered more probable than the non-unique second forbidden one and in this work the Fermi plot corresponding to the former transition has been used to calculate the intensity value of the transition.

To find the intensity of the transition, the Fermi plot (Line II of Figure 6) was extrapolated back to zero energy. This provided the

counting rates expected in the β-spectrum in the energy regions not experimentally studied. A β-spectrum was then plotted, followed by a comparison of the area underneath with that of the internal conversion line of the 1.332 Mev transition. The intensity of the β-transition was then deduced from the known conversion coefficient of the line. The procedure yielded an intensity value of 0.925×10^{-4} beta ray per disintegration.

Using Feenberg and Trigg's curves, the value of comparative half-life is found as $\log f_o t = 13.95$. This value used in Davidson's relations given in Page 9 yields a value for $\log f_2^3 t$ as 13.06.

The results of our measurements agree well with that of J. L. Wolfson. Like us he used only the high energy tail of the spectrum. In Figure 5, the counting rates inbetween the 1.17 and 1.33 Mev conversion peaks have been drawn 200 times larger and compared with that expected which would join smoothly with the high energy tail. The much higher counting rate in this region can be accounted for mostly by the scattered electrons from the fairly thick source backing and spectrometer walls by the intense 1.33 Mev γ flux. Any attempt to calculate the intensity of the transition using the β-spectrum between the conversion peaks and below those will definitely give much higher values like Keister and Langer et al found.

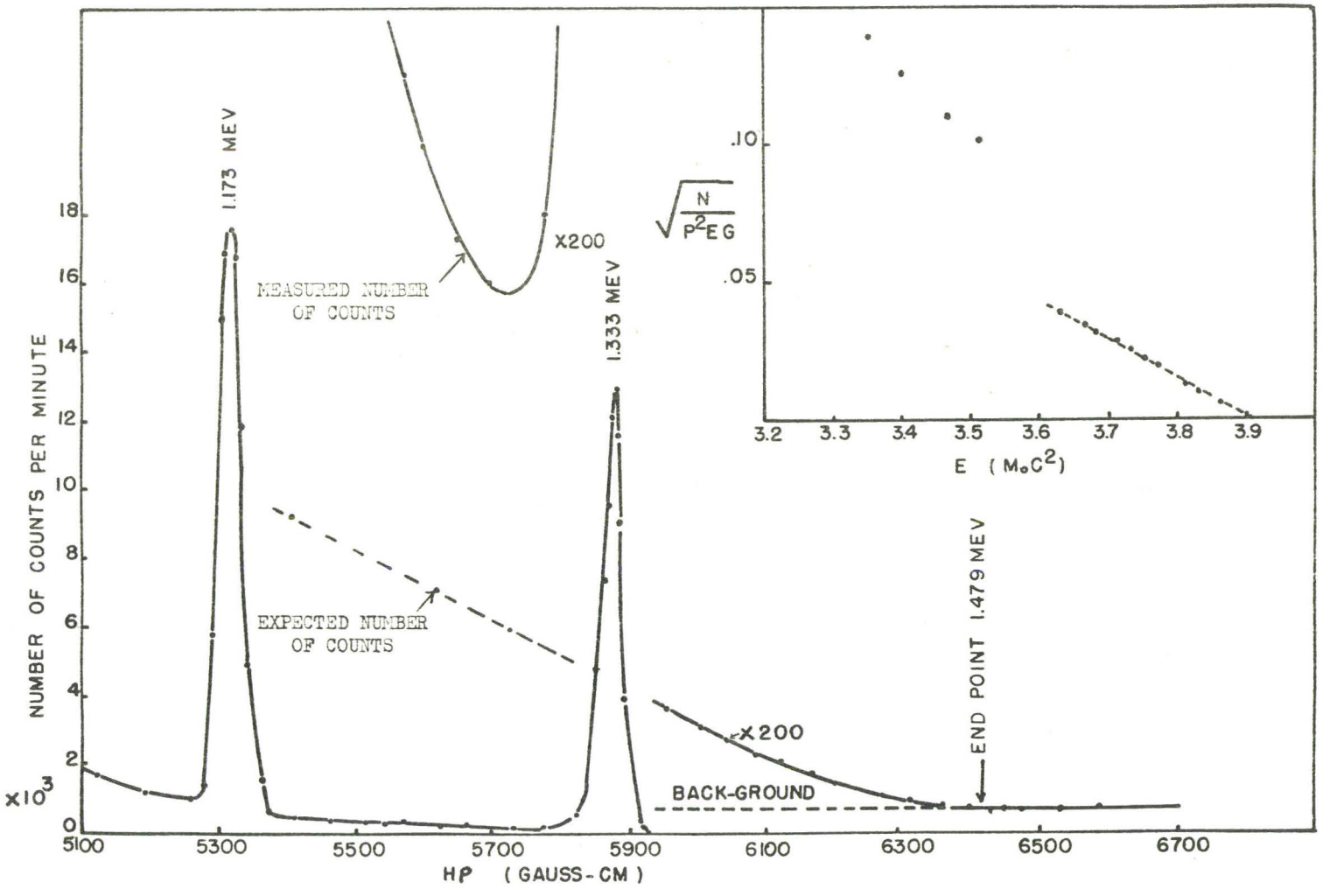
1.173 MEV
1.333 MEV
X200
MEASURED NUMBER OF COUNTS
EXPECTED NUMBER OF COUNTS
X200
BACK-GROUND
END POINT 1.479 MEV
NUMBER OF COUNTS PER MINUTE
X10³
HP (GAUSS-CM)
5100
5300
5500
5700
5900
6100
6300
6500
6700
0
2
4
6
8
10
12
14
16
18
.10
.05
E (M₀C²)
3.2
3.3
3.4
3.5
3.6
3.7
3.8
3.9

FIGURE 5

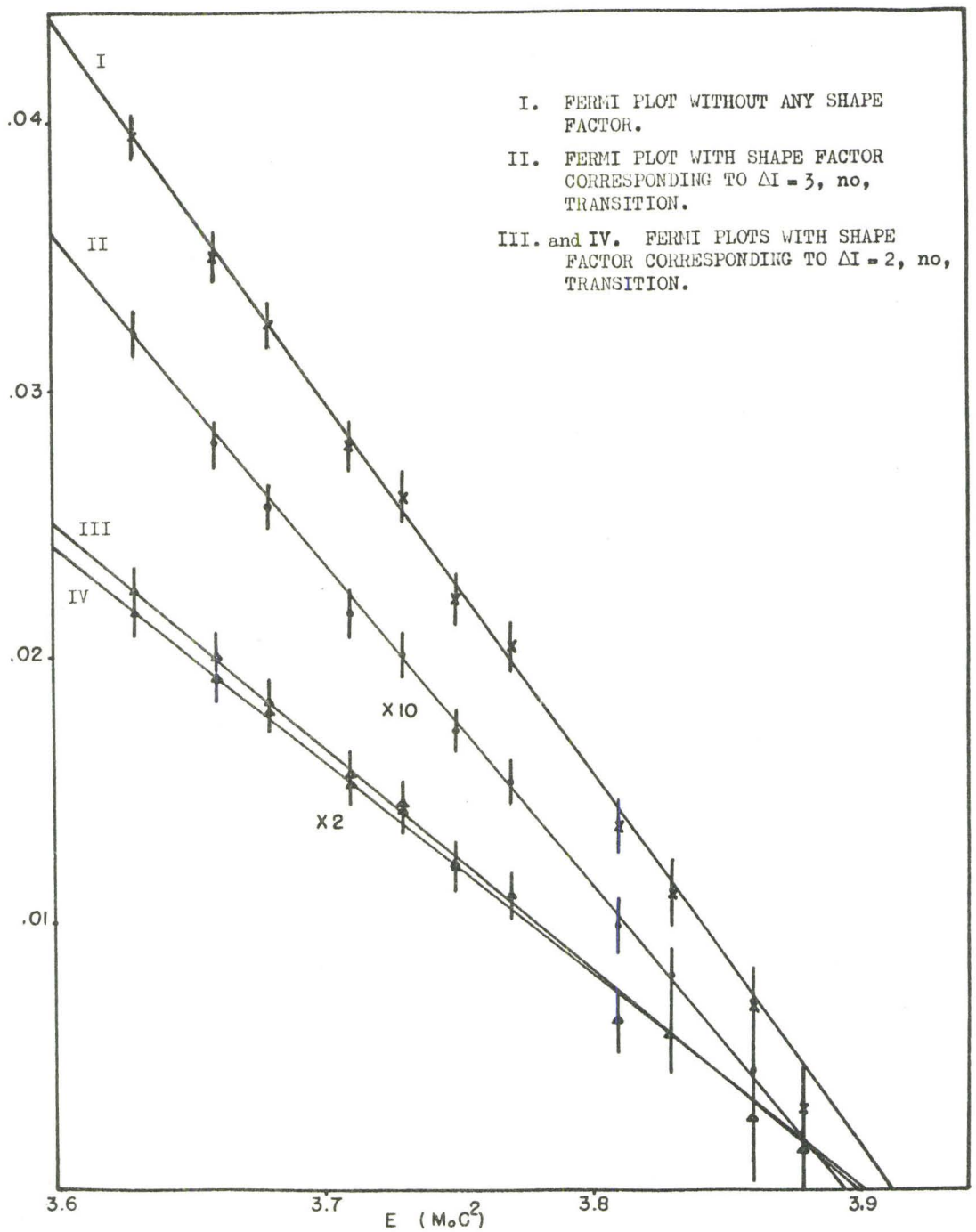
I
II
III
IV
X10
X2
.04
.03
.02
.01
3.6
3.7
3.8
3.9
E (M₀C²)
I. FERMI PLOT WITHOUT ANY SHAPE FACTOR.
II. FERMI PLOT WITH SHAPE FACTOR CORRESPONDING TO ΔI = 3, no, TRANSITION.
III. and IV. FERMI PLOTS WITH SHAPE FACTOR CORRESPONDING TO ΔI = 2, no, TRANSITION.

FIGURE 6

DETECTION OF THE 2.158 AND 0.346 MEV GAMMA RAYS

Introduction

Fluharty and Deutsch[15] in 1949 detected some rare γ-rays from several sources including Co^{60} by observing the photoneutrons produced in masses of Be^{9} and H^{2} surrounding the gamma ray source. Since the threshold γ energy for production of neutrons in Be^{9} is 1.63 Mev and that in H^{2} is 2.23 Mev, they were able to show that the high energy radiation from Co^{60} had an energy $1.63 < E < 2.23$ Mev and an intensity of about 10^{-5} per disintegration. The fact that no neutrons were observed with the H^{2} target indicates that the 2.505 Mev cross-over transition between the strongly populated 4^{+} state at 2.505 Mev and ground has an intensity less than this figure. In fact, it has never been observed.

Nussbaum et al[16] observed gamma-gamma coincidences between the 0.85 Mev and 1.33 Mev gamma-rays in the decay of 24.6 minute Cu^{60} in Ni^{60}. They postulated the existence of 2.158 level in Ni^{60} and actually found the γ ray of energy 2.13 ± 0.4 Mev corresponding to the cross over transition from this level to the ground state of Ni^{60}. The authors proposed an assignment of 2^{+} for the 2.159 Mev level. In this case, this level ought to be fed by a γ ray of energy 0.346 Mev from the 2.505 Mev level in Ni^{60}.

Wolfson[17] made a search for both the 2.158 and 0.346 Mev γ rays with a strong 150 mc Co^{60} gamma source. With a uranium radiator, the

photoelectron line at 2.043 Mev was interpreted as the K-line due to γ-ray of energy 2.158 ± 0.005 Mev. The intensity of the transition he found to be $(1.2 \pm 0.2) \times 10^{-5}$ per disintegration. Wolfson's attempt to observe the 0.346 Mev γ ray was not successful.

With the strong Co^{60} beta source previously described, internal conversion peaks of both the 2.159 Mev and 0.346 Mev γ rays were observed in our laboratory.

The Experiment and Results

The Internal Conversion Peak of 2.159 Mev γ-Transition

The 1 cm thick plastic crystal coated with aluminum foil and the duMont 6292 photomultiplier tube was used as the detector in the Siegbahn type spectrometer.

A very low background was required to observe the internal conversion peak of the 2.159 Mev γ-ray. With the baffles wide open, adjustment of the high voltage for the photomultiplier tube reduced the background to about 5 counts/min. A single channel pulse height analyzer used in the counting circuit reduced the background to 0.25 counts/min. The position of the lower level discriminator was calibrated by setting the analyzer on the conversion peak of 1.333 Mev transition and on the different energy regions of the β-continuum where the counting rates were high due to the intense Compton electrons.

With the low background, the internal conversion peak of the gamma ray was quite prominant and is shown in Figure 7. Calibrating with the internal conversion line of 1.333 Mev transition, the energy of the peak is found to be 2.156 ± 0.003 Mev. The intensity of the

transition is obtained in the manner explained on Page 17, by comparison with the same conversion line of the 1.333 Mev γ transition. Using Rose's tables[18] for the necessary internal conversion coefficients for the E2 transitions, the intensity of the 2.156 $\pm$ 0.003 Mev transition is found to be 1.31×10^{-5} per disintegration.

The fact that the present measurement using internal conversion in nickel and Wolfson's measurement using external conversion in uranium lead to the same transition energy is conclusive proof that this transition belongs to the Co^{60} decay pattern and is not an impurity.

The Internal Conversion Peak of the 0.346 Mev γ-Transition

The detector used in the spectrometer was a 3 mm thick anthracene crystal with the duMont 6292 photomultiplier tube.

The internal conversion peak of the 0.346 Mev γ ray shown in Figure 7 was found as a hump on the spectrum of scattered electrons just above the beta end point of the intense 309 kev beta group. Despite the background, the peak offers conclusive evidence to the existence of the gamma ray. The peak was replotted subtracting the background. Again using the K-conversion line of 1.333 Mev transition, the energy value was found to be 0.345 $\pm$ 0.001 Mev, while the intensity was $5.6 \pm 1 \times 10^{-5}$ per disintegration calculated in the manner explained earlier. The errors on both the energy and intensity of this line was rather large because of the uncertainties in the rapidly changing background.

The energy value of the K-conversion peak observed is a little lower than the predicted value. The following reasons may account for this.

The background level of the peak is drawn by joining smoothly the counting rates preceeding and following the peak. But the presence of the L peaks of the transition around $H\rho$ = 2279, will raise the background on the higher energy side of the K-peak. This will in effect shift the peak position to the lower energy side giving a lower energy value. An attempt to correct for this effect has been made.

Further at this low energy region, the source thickness effect will be more prominant. For a thick source, the lower energy edge of the peak will be smeared out with an apparent shifting of the peak position to the lower energy side. We had a fairly thick source of thickness about 600 u gm/cm^2. This had no effect on the higher energy peaks measured before but would be expected to cause some tailing on the low energy side of this peak. That this was not very serious is indicated by the fact that the resolution is about 0.8%, only little higher than the instrumental resolution.

In Ni^{60}, the 0.346 Mev γ transition proceeding from the 2.505 Mev (4^+) level feeds the 2.159 Mev $(2^{(+)})$ level. The latter level subsequently decays down to the 1.333 Mev (2^+) level and to the ground state (0^+) by γ transitions with energies 0.827 and 2.159 Mev respectively. Besides the 0.346 Mev γ ray, the 2.159 Mev level is fed from the ground state of Co^{60} by an extremely weak 0.656 Mev β-ray, which cannot account for more than a small fraction of the intensities of the 0.827 and 2.159 Mev γ rays. So, from the intensities of the 0.346 Mev and 2.159 Mev γ rays, it is possible to predict an intensity value for the 0.827 Mev transition and from our measurements it is predicted as 4.3×10^{-5} per disintegration. This gives the ratio of the intensities of the

0.827 Mev and 2.158 Mev γ rays as 3.31:1. This value may be compared with the value 2.66:1 as measured by Nussbaum et al by scintillation counter. Due to the high flux of Compton electrons, search for the 0.827 Mev conversion peak proved impracticable.

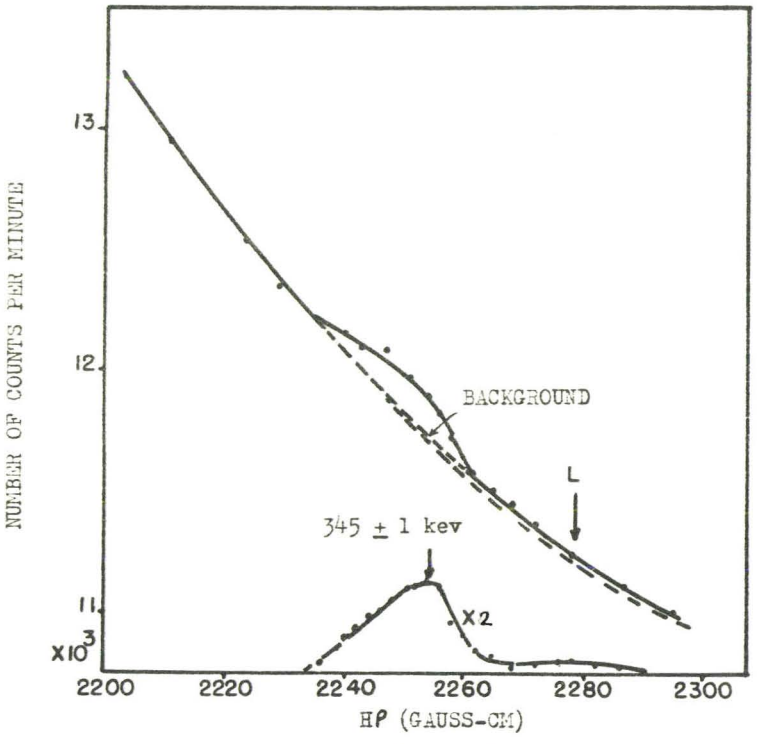

FIGURE 8

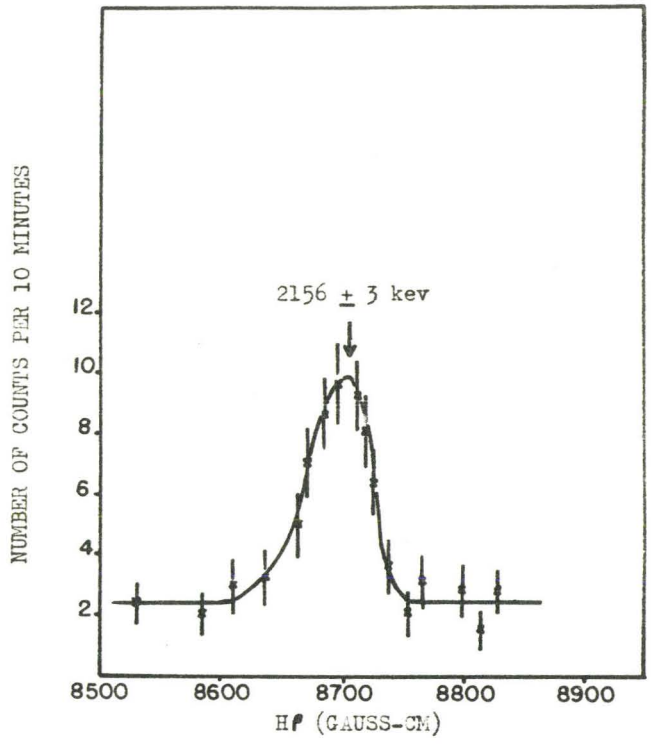

FIGURE 7

APPENDIX

Shape Factor for the Second Forbidden Unique Beta Transition

The unique transitions which arise only from the Gamow-Teller interaction, the shape factors, can be calculated exactly. For a nth forbidden unique transition, for which $\Delta I = n + 1$, the shape factor S_n^{n+1}, is given by

$$S_n^{n+1} \sim \sum_{\nu=0}^{n} \frac{(2n+1)!}{(2\nu+1)!(2n-2\nu+1)!} p^{2\nu} q^{2(n-\nu)}$$

where $p = (E_o^2 - 1)^{1/2}$, the electron momentum and $q = E_o - E$, the neutrino energy (which is the same as the neutrino momentum in the units used).

When the Coulomb effect on the electron is taken into account, the above expression is modified to

$$Sn^{n+1} \sim \sum_{\nu=0}^{n} \frac{(2n+1)!\,(2\nu+1)!}{2^{2\nu}(\nu!)^2(2n-2\nu+1)!} q^{2(n-\nu)} L_\nu$$

where L_ν is a tabulated function given explicitly by Greuling[6]. For $A<100$, a good approximation for L_ν is

$$L_\nu = \alpha_\nu{}^2 p^{2\nu} \quad \text{with} \quad \alpha_\nu = \frac{2^\nu \nu!}{(2\nu+1)!}$$

Applying the formula to n = 2 leads to the shape factor for the second forbidden unique transition

$$S_2^3 \sim p^4 + \frac{10}{3} p^2 q^2 + q^4.$$

Shape Factor for the Second Forbidden Non-Unique Transition

For a second forbidden non-unique transition for which $\Delta I = 2$, the shape factor can be deduced[18] as

$$S_2^2 \sim p^2 + \lambda q^2$$

where $\lambda = \frac{4 (1 - \epsilon x \xi + \epsilon x \eta)^2}{(1 - \epsilon x \xi + 2 \epsilon x \eta)^2}$,

with $\epsilon = -1$ for electron emission, and $x = g_V/g_A$, the ratio of the interaction constants and equal to $-1/1.24$. Parameters ξ and η in the expression for λ are defined as

$$(f \| y_n (r) \| i) = - i \xi_n (f \| T_n (n, \sigma) \| i)$$

and

$$(f \| T_n (n-1, \alpha) \| i) = \eta_n \frac{\alpha Z}{2R} (f \| T_n (n, \sigma) \| i)$$

where i and f refer to the initial and final states respectively and y_n, T_n are the spherical tensors.

The values of ξ and η have to be calculated from the knowledge of the wave functions of the states and are quite difficult to find. But it is found that their values remain near ± 1. Therefore, taking ξ and η as ± 1, the values of λ can be calculated and applied to give the non-unique shape factors presented below.

The appropriate shape factors are then

$$S_2^2 \sim p^2 + 0.747\, q^2 \text{ for } \xi = +1,\ \eta = -1$$
$$\sim p^2 + 1.23\, q^2 \text{ for } \xi = +1,\ \eta = +1$$
$$\sim p^2 + 2.34\, q^2 \text{ for } \xi = -1,\ \eta = +1$$
$$\sim p^2 + 106.3\, q^2 \text{ for } \xi = -1,\ \eta = -1.$$

Since q is small over the entire high energy range of the Co^{60} spectrum available for experimental investigation, the term involving q^2 is relatively unimportant and it is not surprising that the shape factors for all values of λ are approximately equal and have the value p^2.

REFERENCES

1. Keister, G. L. and Schmidt, F. H., Phys. Rev. 93, 140 (1954).

2. Wolfson, J. L., Can. J. Phys. 34, 256 (1956).

3. Camp, D. C., Langer, L. M. and Smith, D. R., Phys. Rev. 123, 24 (1961).

4. Fermi, E., Z. Physik 88, 161 (1934).

5. Rose, M. E., Tables of Fermi Functions, Appendix II, "Beta and Gamma Ray Spectroscopy", Edited by K. Siegbahn, North-Holland Publishing Company, Amsterdam.

6. Greuling, E., Phys. Rev. 61, 568 (1942).

7. Konopinsky, E. J., Chapter X, "Beta and Gamma Ray Spectroscopy", Edited by K. Siegbahn.

8. Davidson, J. P., Phys. Rev. 82, 48 (1951).

9. Feenberg, E. and Trigg, G., Rev. Mod. Phys. 22, 399 (1950).

10. Johns et al., Can. J. Phys. 31, 225 (1953).

11. Schull, F. B. and Dennisson, D. M., Phys. Rev. 71, 681 and 72, 256 (1947).

12. Dunn, R. W., Nucleonics 7 and 8, 10 (1952).

13. Safranek, W. H. and Winkler, J. H., Page 231, Modern Electro-Plating, A. G. Gray, John Wiley and Sons, New York.

14. Dobrowolsky, W. Jones, R. V. et al., Phys. Rev. 101, 1001 (1956).

15. Fluharty, R. G. and Deutsch, M., Phys. Rev. 76, 182 A (1949).

16. Nussbaum, R. H. et al., Physica 20, 555 (1954).

17. Wolfson, J. L., Can. J. Phys. 33, 886 (1955).

18. Preston, M. A., Chapter 15, Physics of the Nucleus, Addison-Wesley Publishing Company, Massachusetts, U.S.A.

19. Sliv, L. A. and Band, I. M., "Coefficients of Internal Conversion of Gamma Radiation", The Academy of Sciences of U.S.S.R.